JOURNAL OF Materials CHEMISTRY

Novel solvothermal synthesis of niobium(v) oxide powders and their photocatalytic activity in aqueous suspensions

Hiroshi Kominami,*[a] Kazuhide Oki,[a] Masaaki Kohno,[a] Sei-ichi Onoue,[a] Yoshiya Kera[a] and Bunsho Ohtani[b]

[a]*Department of Applied Chemistry, Faculty of Science and Engineering, Kinki University, Kowakae, Higashiosaka, Osaka, 577-8502, Japan. E-mail: hiro@apch.kindai.ac.jp*
[b]*Catalysis Research Center, Hokkaido University, Sapporo 060-0811, Japan*

Received 22nd June 2000, Accepted 30th October 2000
First published as an Advance Article on the web 18th December 2000

Niobium(v) oxide (Nb_2O_5) powders were synthesized by the solvothermal reaction of niobium(v) pentabutoxide (NPB) in toluene at 573 K in the absence or presence of water. Nb_2O_5 powder with a large surface area ($>200\ m^2\ g^{-1}$) was obtained in the absence or presence of only a small amount of water. Its X-ray diffraction (XRD) pattern showed no clear peaks, and the Raman spectrum suggested formation of an Nb–O–Nb network, *i.e.*, an amorphous Nb_2O_5 structure without long-range order. A further increase in the amount of water used in the synthetic procedure induced crystallization of Nb_2O_5 into the TT-phase. The surface area of the solvothermal products decreased with increases in the amount of water used, indicating growth of particles *via* water-induced extension of the Nb–O–Nb network. These Nb_2O_5 particles were platinized and then used for photocatalytic dehydrogenation of methanol in an aqueous solution under deaerated conditions. The amorphous Nb_2O_5 produced by the solvothermal process exhibited a rate of hydrogen evolution higher than that of the crystalline Nb_2O_5 samples or other amorphous Nb_2O_5 samples supplied as niobic acid ($Nb_2O_5{\cdot}nH_2O$) and those prepared by hydrolysis of NPB under atmospheric conditions. Photocatalytic mineralization of acetic acid in aqueous solution was also conducted with bare Nb_2O_5 under aerated conditions. The amorphous Nb_2O_5 samples, especially catalysts prepared by the solvothermal method, exhibited a rate of carbon dioxide formation much higher than that of the crystalline Nb_2O_5 samples also used in this photocatalytic reaction system.

Introduction

Fundamental studies on the photocatalysis of titanium(iv) oxide (TiO_2) and its applications have been extensive due to the high activity and stability of TiO_2 as well as the wide-ranging availability of photocatalytic systems.[1–5] Other metal oxides such as tungsten(vi) oxide (WO_3),[6] zirconium(iv) oxide (ZrO_2),[6] potassium niobate ($K_4Nb_6O_{17}$),[7] potassium tantalate ($KTaO_3$)[8] and barium titanate ($BaTi_4O_9$)[9] and sulfides, *e.g.*, cadmium sulfide (CdS)[10] and zinc sulfide (ZnS),[11] were also found to exhibit photocatalytic activity for a large number of reaction systems. Among the metal oxides, niobium(v) oxide (Nb_2O_5) has a band gap energy of 3.4 eV, similar to TiO_2 (3.2 eV), and, therefore, it would be expected to have photocatalytic activity similar to TiO_2. However, there have been few reports on photocatalysis by Nb_2O_5. Since the potential conduction band edge of Nb_2O_5 was reported to lie close to the H^+/H_2 (0 V at pH 0) redox potential, it is also an interesting point whether an Nb_2O_5 photocatalyst can produce H_2 from water or not.

In the course of studies on the synthesis of inorganic materials in organic media,[12–15] we found that nano-crystalline anatase TiO_2[16,17] and iron oxides (α-Fe_2O_3 and Fe_3O_4)[18] were synthesized by solvothermal treatment of alkoxides or acetylacetonate in organic media at around 573 K. These products possessed both high crystallinity and a large surface area. On the basis of kinetic investigation of the photocatalytic reaction of TiO_2, it has been pointed out that TiO_2 powders satisfying these two properties should show higher photocatalytic activity.[19] As expected, the TiO_2 nano-particles synthesized in organic media exhibited photocatalytic activity much higher than those of commercially available active TiO_2 for several reaction systems, including H_2 evolution from aqueous solution of propan-2-ol,[20] oxygen evolution from silver sulfate solution,[20,21] deamino-N-cyclization of (*S*)-lysine,[22] and mineralization, *i.e.*, complete decomposition of acetic acid in aqueous solutions.[23]

In the present study, we applied the solvothermal method for the synthesis of Nb_2O_5 and thus-obtained Nb_2O_5 samples were used for photocatalytic dehydrogenation of methanol in aqueous solution under deaerated conditions and mineralization of acetic acid under aerated conditions. We also investigated the correlation between the properties and photocatalytic activity of Nb_2O_5.

Experimental

Solvothermal synthesis of Nb_2O_5

Niobium pentabutoxide (NPB, Kanto Chemical, 4 g) was dissolved in toluene (90 cm^3) in a test tube, which was then set in a 500 cm^3 autoclave (Fig. 1). 60 cm^3 of toluene (or water) was placed in the gap between the test tube and inside wall of the autoclave. The autoclave was thoroughly purged with nitrogen, heated to 573 K at a rate of 2.5 K min^{-1}, and kept at that temperature for 2 h. After heating, the resulting powder was washed repeatedly with acetone and dried in air at room temperature. Calcination of the sample was carried out in a box furnace; the sample was heated to the desired temperature in a combustion boat at a rate of 10 K min^{-1} and kept at that temperature for 1 h.

 DOI: 10.1039/b008745i

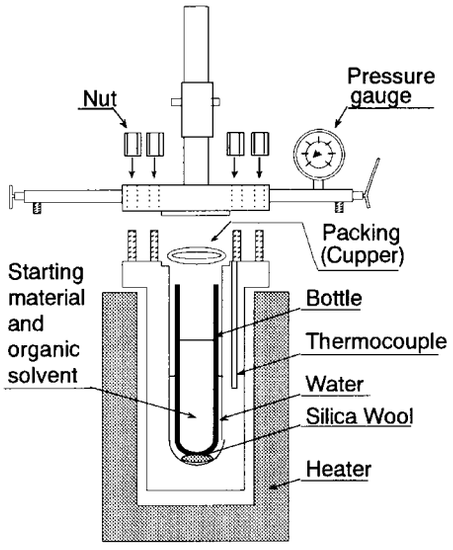

Fig. 1 Reaction apparatus.

Characterization

Powder X-ray diffraction (XRD) patterns were recorded on a Rigaku RINT 2500 equipped with a carbon monochromator (CuKα radiation). Thermogravimetry (TG) and differential thermal analysis (DTA) were performed using a Rigaku TG-8120 with an air flow of 100 cm^3 min^{-1}. The morphology of the products was observed using a JEOL JEM-3010 transmission electron microscope (TEM), operated at 300 kV, in the Joint Research Center, Kinki University. FT Raman spectra were recorded on a Nicolet Raman 950 with a 20 mW YAG laser (1064 nm). The spectra of 500 scans were accumulated with 4.0 cm^{-1} resolution. Diffuse reflectance spectra were obtained with a Shimadzu UV-2400 UV-vis spectrometer equipped with a diffuse reflectance measurement unit (ISR-2000) and recorded after Kubelka–Munk analysis. The specific surface area was calculated by the BET single-point method from nitrogen uptake at 77 K.

Photocatalytic dehydrogenation of methanol in an aqueous suspension of Nb_2O_5 under deaerated conditions

Photocatalytic activity of Nb_2O_5 for the dehydrogenation of methanol in a deaerated aqueous solution was carried out according to the method described in previous papers with some modifications.[14,15,20,24] Pre-treatment was carried out to decompose contaminated organic moieties on the Nb_2O_5 surface; Nb_2O_5 powder (*ca.* 200 mg) was suspended in 5 cm^3 of water and photoirradiated at a wavelength of >300 nm by a high-pressure mercury arc (400 W) under oxygen with magnetic stirring until no more carbon dioxide was liberated. Then the Nb_2O_5 powder was recovered and dried under air at 323 K. The Nb_2O_5 powder (50 mg) was again suspended in water (2.5 cm^3) in a test tube, argon was bubbled into the suspension for 30 min, and then the tube was sealed with a rubber septum. Platinum (0.5 wt%) was deposited on Nb_2O_5 particles by the photodeposition method; an aqueous solution of tetraammineplatinum(II) chloride ($[Pt(NH_3)_4]Cl_2$, Wako Pure Chemical) was injected into the tube through a rubber septum, and was then photoirradiated under the same irradiation conditions for 2 h. After platinization, 2.5 cm^3 of methanol was dissolved in the suspension to form 50 vol% methanol solution, and Ar was bubbled through the sample again. The tube was sealed and photoirradiated under the same conditions as those described above. The amount of H_2 in the gas phase was measured every hour using a Shimadzu GC-8A gas chromatograph equipped with an MS-5A column.

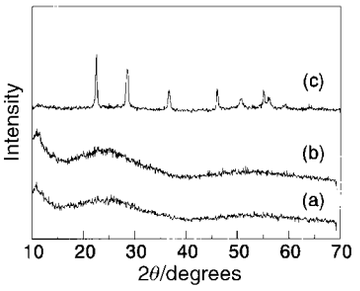

Fig. 2 XRD patterns of the products obtained by the thermal treatment (573 K for 2 h) of niobium(V) pentabutoxide (NPB) in toluene (a) in the absence of water (NB-0), and in the presence of (b) 5 cm^3 (NB-5), and (c) 30 cm^3 (NB-30) of water.

Photocatalytic mineralization of acetic acid in an aqueous suspension of Nb_2O_5 under aerated conditions

The pre-treated and dried Nb_2O_5 powders (50 mg) were suspended in 5 cm^3 of water, and air was bubbled into the suspension for 30 min. After the test tube had been sealed with a rubber septum, acetic acid (175 μmol) was injected.[14,15,23] The resulting aerated aqueous suspension was irradiated at 298 K. The amount of CO_2 in the gas phase was measured every hour using a Shimadzu GC-8A gas chromatograph with a Porapak QS column.

Results and discussion

Characterization of Nb_2O_5 synthesized by the solvothermal method

Fig. 2 shows XRD patterns of products obtained by the solvothermal process. A powder prepared in the absence of water (NB-0) gave no sharp peaks, *i.e.*, it was amorphous. Since the addition of water to a supernatant of NB-0 after autoclaving gave no precipitates, NPB would have been almost completely consumed during the process. The presence of a small amount of water (5 cm^3) fed into the gap between the test tube and the autoclave wall instead of toluene (see Fig. 1) also resulted in the formation of an amorphous product (NB-5). When a larger amount of water (30 cm^3) was fed into the gap, crystalline Nb_2O_5 in the TT-phase,[25] which is one of the kinetically stabilized phases of Nb_2O_5, was obtained (NB-30).

TEM photographs of these three products are shown in Fig. 3. NB-0 consisted of very small particles of less than 3 nm in diameter, the particle size of NB-5 was slightly larger than that of NB-0. In contrast to the amorphous products, prismatic crystals were observed in the photograph of NB-30, presumably corresponding to the TT-phase crystallites.

The results of thermal analysis of the three products are shown in Figs. 4 and 5. In the TG curves (Fig. 4), weight loss, attributed to desorption of physically adsorbed water and elimination of organic moieties on and/or in the products, was observed from room temperature to 723 K for all products, while only negligible weight loss was seen in the temperature range of 723 to 1273 K. It is clear that the increase in the amount of water added to the reaction apparatus decreased the weight loss up to 723 K (Table 1), suggesting elimination of organic moieties from Nb_2O_5 is accelerated by water. In the DTA curves (Fig. 5), an endothermic peak below 373 K and exothermic peaks at around 523 and 673 K were seen. These endothermic and exothermic peaks are due to desorption of water and combustion of organic moieties, respectively. Other exothermic peaks with negligible weight loss were observed at 846 and 867 K in the curves of NB-0 and -5, respectively, and these are assigned to crystallization of the amorphous phase into the TT-phase as discussed later.

In the Raman spectra (Fig. 6) of NB-0 and -5, three bands were observed at around 230, 650 and 915 cm^{-1}, resembling

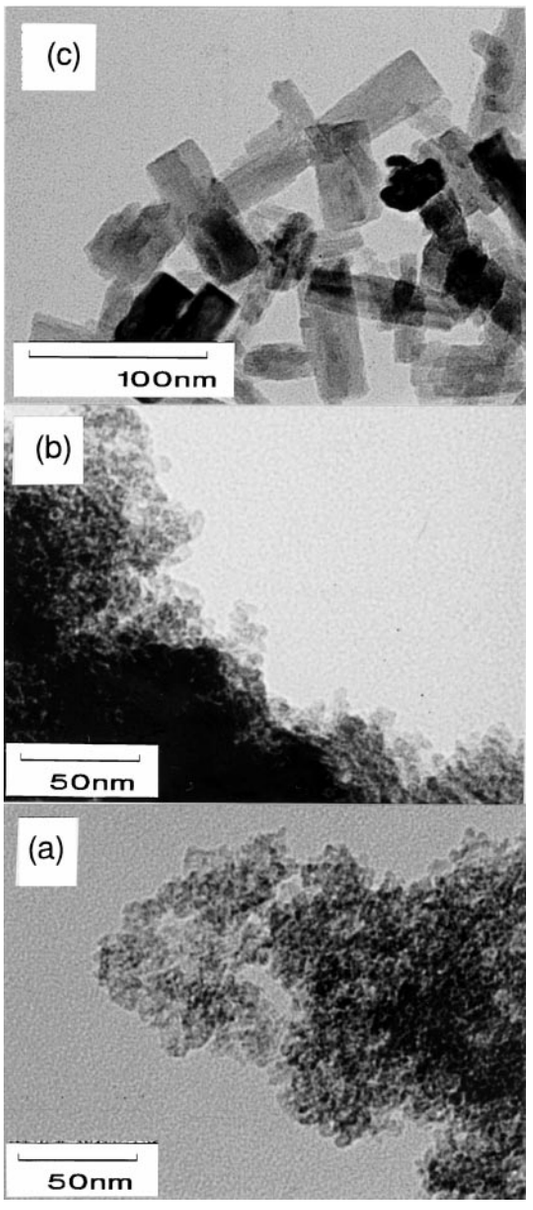

Fig. 3 TEM photographs of (a) NB-0, (b) NB-5, and (c) NB-30.

commercial hydrated Nb_2O_5 ($Nb_2O_5{\cdot}nH_2O$)[26] and xerogel Nb_2O_5 prepared by hydrolysis of niobium(v) chloride.[27,28] Jehng and Wachs[26] have assigned these three bands to the bending of Nb–O–Nb linkages, symmetric Nb–O stretching of Nb_2O_5 polyhedra, and the symmetric stretching of surface Nb=O, respectively. The broadness of these may reflect the distribution of slightly distorted NbO_6, NbO_7, and NbO_8 polyhedra in the amorphous Nb_2O_5.[29] On the other hand, NB-30 gave an intense peak at 716 cm^{-1} and weak ones at 323 and 250 cm^{-1}, which are consistent with the reported TT-phase Nb_2O_5 characteristics.[26,28]

Table 1 summarizes the physical properties of the Nb_2O_5 samples. NB-0 possessed a large surface area of 350 $m^2\ g^{-1}$, which corresponds to a very small spherical particle size (<3 nm) as observed in TEM photographs, while NB-5 showed a smaller surface area. The decrease means that water dissolved in organic solvent accelerates extension of the Nb–O–Nb network, *i.e.*, growth of Nb_2O_5 particles. Further addition of water induced the formation of TT-phase crystallites of smaller surface area (NB-30). Our previous studies[16,17] using the solvothermal method under similar conditions have clarified that water in the gap is vaporized and dissolved in toluene during the thermal treatment. In the absence of added

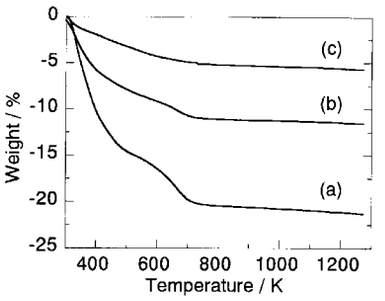

Fig. 4 TG curves of (a) NB-0, (b) NB-5, and (c) NB-30.

water, the lower solubility of Nb_2O_5 in toluene prohibits the growth of particles *via* a dissolution–recrystallization mechanism to give the small particle size of NB-0. The more water added, the greater the water content in the reaction medium and, therefore, the greater the solubility of Nb_2O_5, resulting in accelerated particle growth and crystallization. For comparison, the physical properties of two commercial Nb_2O_5 samples, one of which is a crystalline T-phase,[30] which is also a kinetically stabilized phase, Nb_2O_5 (Wako Pure Chemical) (NB-A) and the other of which is amorphous Nb_2O_5 supplied as niobic acid ($Nb_2O_5{\cdot}nH_2O$, Mitsuwa Chemical) (NB-B) are also listed in Table 1. Another amorphous Nb_2O_5 sample was prepared by hydrolysis of NPB in alcoholic solution under atmospheric pressure (NB-C). NB-A possessed a very small surface area, reflecting its well-crystallized nature. Amorphous NB-B and -C showed larger surface areas compared with that of NB-A. The differences between the amorphous powders prepared by the solvothermal process (NB-0, -5) and those obtained commercially (NB-B, -C) will be discussed in the following section.

Fig. 7 and Table 1 show XRD patterns and physical properties of samples obtained by calcination of NB-5 at various temperatures, respectively. Apparently no change could be seen in the XRD pattern when calcined at 573 K, whereas TT-phase Nb_2O_5 appeared by calcination at 823 K. This observation is consistent with the detection of an exothermic peak in the DTA (Fig. 4) assigned to a transformation from an amorphous to the TT-phase. The TT sample, NB-5-823, possessed a larger surface area of 111 $m^2\ g^{-1}$ compared with those of the other TT powders (NB-30 and calcined commercial samples, NB-B-823 and NB-C-823). The TT-phase was transformed into the T-phase on calcination at 973 K accompanied by a marked decrease in surface area.

The crystallization temperature of the TT-phase (T_{cry}) obtained from the DTA curves is shown in Table 1; T_{cry} was in the order of NB-C < NB-0 < NB-5. Since T_{cry} can be a semi-quantitative measure of stability of short-range order in the Nb–O–Nb network, the higher T_{cry} of NB-5 than NB-C of a similar surface area or NB-0 prepared under similar conditions suggests an even higher order of structure in NB-5, though XRD patterns indicate only an amorphous phase. Further support of the relatively higher order of the NB-5 structure is

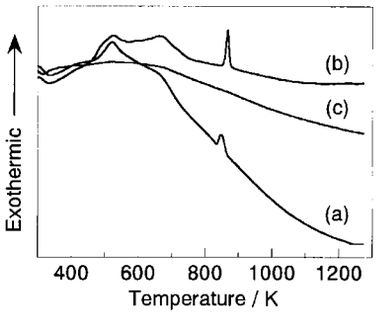

Fig. 5 DTA curves of (a) NB-0, (b) NB-5, and (c) NB-30.

Table 1 Physical properties and photocatalytic activity of Nb_2O_5 powders synthesized under various conditions

Nb_2O_5 sample	Water[a]/ cm^3	T_{cal}[b]/K	Primary particle	Phase[c]	Weight loss[d](%)	T_{cry}[e]/K	$S_{BET}/m^2\ g^{-1}$	λ_{edge}[f]/nm	H_2[g]/ $\mu mol\ h^{-1}$	CO_2[h]/$\mu mol\ h^{-1}$
NB-0	0	—	Sphere < 3 nm	Amorphous	20.1	846	350	358	23	5.3
NB-5	5	—	Sphere ~ 5 nm	Amorphous	10.7	867	252	355	56	5.4
NB-5-723	5	723		Amorphous	—	—	232	—	35	4.2
NB-5-823	5	823		TT	—	—	111	363	35	3.3
NB-5-973	5	973		T	—	—	28	365	9	1.8
NB-5-1123	5	1123		T	—	—	< 1	nd	1.1	nd
NB-30	30	—	Prism 30 × 60 nm	TT	4.9	—	57	357	4	2.3
NB-A[i]	—	—		T		—	5	370	1	1.1
NB-B[j]	—	—		Amorphous			82	334	25	2.6
NB-B-823	—	823		TT	—	—	30	349	6	< 1
NB-C[k]	—	—		Amorphous	17.4	842	221	338	32	3.3
NB-C-823	—	823		TT	—	—	33	371	4	1.2
(TiO_2)[l]	—	—		Amorphous	—	—	—	—	8	—

[a]The amount of water fed into the gap between the test tube and the autoclave wall. [b]The sample was calcined at T_{cal} for 1 h. [c]Determined by X-ray diffraction (XRD) and Raman spectra. [d]Weight loss up to 773 K. [e]Crystallization temperature determined from the DTA curve. [f]Absorption edge in absorption spectrum. [g]Rate of hydrogen evolution from an aqueous solution of 50 vol% methanol (5 cm^3) in the presence of photoirradiated platinum (0.5 wt% to Nb_2O_5). [h]Rate of carbon dioxide evolution from an aqueous solution (5 cm^3) of acetic acid (175 μmol). [i]Supplied by Wako Pure Chemical. [j]Supplied by Mitsuwa Chemical as niobic acid, $Nb_2O_5 \cdot nH_2O$. [k]Prepared by hydrolysis of niobium pentabutoxide under atmospheric conditions. [l]Supplied by Wako Pure Chemical as amorphous titanium oxide.

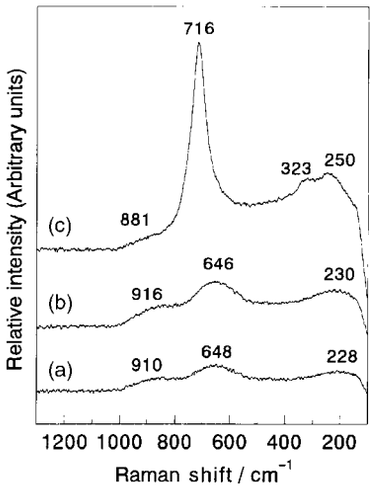

Fig. 6 Raman spectra of (a) NB-0, (b) NB-5, and (c) NB-30.

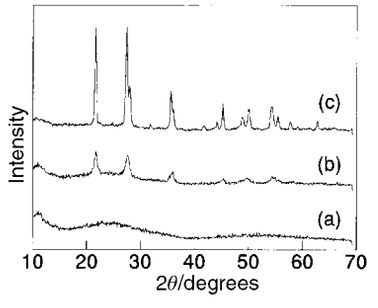

Fig. 7 XRD patterns of samples obtained by calcination of NB-5 at (a) 573 K, (b) 823 K, and (c) 973 K.

the longer wavelength absorption edge. Fig. 8 shows representative absorption spectra of Nb_2O_5 samples. The wavelength of the absorption edge, calculated for convenience by extrapolation of a linear part of the absorption rise, was in the range of 330–370 nm, as shown in Table 1, which was almost the same or a little shorter than that reported for crystalline Nb_2O_5 (365 nm; 3.4 eV). As a general trend, crystallization of amorphous samples on calcination at a higher temperature induced a red shift of the absorption edge. While the commercial amorphous samples (NB-B) give the shortest edge wavelength, NB-0 and $5Nb_2O_5$ show intermediate values around 360 nm, presumably due to a quantum-size effect.[31–33] The crystalline samples, except for NB-B-823, show the longest wavelength. At present, we can not explain the change in the edge wavelength, but it is clear that NB-5 (and NB-0) behaves like a crystalline rather than an amorphous material.

Photocatalytic dehydrogenation of methanol under deaerated conditions and mineralization of acetic acid under aerated conditions

Fig. 9 shows the time course of H_2 evolution from an aqueous suspension of bare and platinized NB-5 powders. A linear increase in H_2 was observed, in both cases, only when the suspension was irradiated. The total molar amount of H_2 liberated by a continuous 5 h irradiation (275 μmol) exceeded the molar amount of Nb_2O_5 used in this experiment (181 μmol). These results clearly indicate that photocatalysis by Nb_2O_5 accounts for the H_2 evolution. The quantum yield of NB-5 under these conditions was roughly estimated to be at least 6%. As can be seen in Fig. 9, bare NB-5 (without platinum loading) also showed an appreciable rate of H_2 evolution(18 $\mu mol\ h^{-1}$). This is in contrast to the case of TiO_2; bare TiO_2 powder exhibits negligible photocatalytic activity for dehydrogenation of alcohols.[24,34,35] The photocatalytic H_2 evolution by bare Nb_2O_5 might be due to the potential of its conduction band edge, which is expected to be a little negative compared with the redox potential of H^+/H_2. In Table 1, the rates of H_2 evolution, calculated from the initial linear part of the time course curve, by various Pt–Nb_2O_5 photocatalysts are summarized. It should be noted that amorphous Nb_2O_5

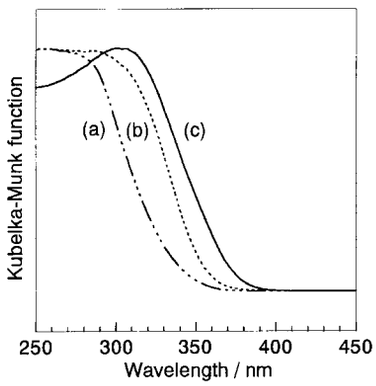

Fig. 8 UV-Vis spectra of (a) NB-B, (b) NB-5, and (c) NB-A.

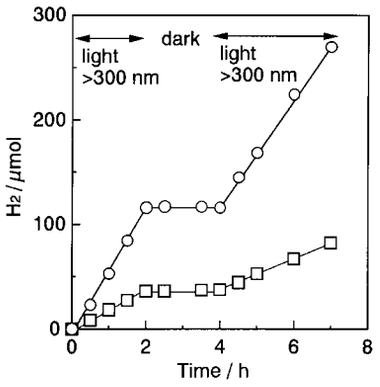

Fig. 9 Time course of hydrogen formation from aqueous methanol solutions of bare NB-5 (squares) and platinized NB-5 (circles).

samples, *i.e.*, NB-0, -5, -B and -C, exhibited faster rates than did crystalline Nb_2O_5 samples, *e.g.*, NB-30 and NB-A. This difference will be discussed in the next section.

Another photocatalytic reaction, mineralization of acetic acid, was operated with these Nb_2O_5 powders; as observed with TiO_2, stoichiometric evolution of carbon dioxide (CO_2) was seen, indicating the reaction of ($CH_3COOH + 2O_2 = 2CO_2 + 2H_2O$). Table 1 shows the initial rate of linear CO_2 evolution. Also in this case, the amorphous samples rather than the crystallized ones showed a faster rate, *e.g.*, NB-5 showed a quantum yield of *ca.* 2%. Fig. 10 is a plot of the rate of CO_2 evolution against one of the physical properties, the BET specific surface area of Nb_2O_5. It seems that the rate of CO_2 evolution depends strongly on the surface area, *i.e.*, the larger the area is, the faster the CO_2 liberation. This is rationalized by the assumption that the photogenerated active species, photoexcited electron (e^-) and positive hole (h^+), react with substrates adsorbed on the surface and the rate of this process(es), in which a larger surface area gives a larger amount of adsorbed substrates,[21] determines the overall photocatalytic activity. It is presumed that the photogenerated e^-–h^+ pair recombine to give no chemical reaction unless it reacts with the substrates and that the rate of recombination depends on the nature of the photocatalyst. Although we have no experimental evidence of recombination rate dependence, it seems clear that the overall photocatalytic reaction rate was mainly controlled by the surface area, not by the crystallinity, which was related to the electron–hole recombination process. For TiO_2 photocatalysts, a similar tendency of activity depending only on their surface area could be seen in the oxidative decomposition of organic compounds under aerated conditions.[14,15,23] However, a commercially obtained amorphous TiO_2 powder (Idemitsu) showed negligible activity even though it has a relatively larger surface area of *ca.* 120 $m^2\ g^{-1}$.[36] As shown in Table 1, another amorphous (or hydrated) TiO_2 from Wako Pure Chemical also showed a much

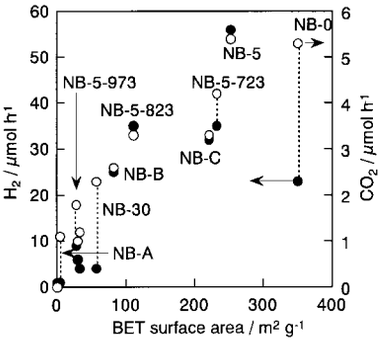

Fig. 10 Dependence of the rate of H_2 (closed circles) and CO_2 (open circles) evolution on the surface area.

slower rate. This is in contrast to the present results for Nb_2O_5 powders, *i.e.*, amorphous but not crystalline particles showed higher activity.

Care should be taken when referring to the structure of amorphous Nb_2O_5, since the term "amorphous" means only no detectable long-range order in the powders and therefore does not specify any structure. In the case of TiO_2, we concluded that the commercial amorphous TiO_2 gives negligible photocatalytic activity because of the enhanced recombination of e^- and h^+ at the defective sites in its structure in spite of the relatively large surface area. Based on this consideration, the relatively higher photocatalytic activity of amorphous Nb_2O_5 samples, especially those as-prepared without post-calcination treatment, *e.g.*, NB-0 and NB-5, which absorb even larger numbers of photons due to the longer wavelength absorption edge, than crystalline particles is attributable to their comparable or even reduced probability of e^-–h^+ recombination. As described in the preceding part of this paper, among the amorphous Nb_2O_5 powders used in this study, the commercial NB-B and NB-C powders showed a much shorter absorption edge wavelength than those obtained *via* the solvothermal process, suggesting their "amorphous" nature. This also leads to a smaller number of absorbed photons. Therefore, it seems reasonable to find that NB-C showed a CO_2-liberation rate a little smaller than expected from the monotonous increase in the activity along with the surface area.

Fig. 10 also shows the dependence of the rate of H_2 evolution from deaerated aqueous methanol on surface area. Although the rate was *ca.* 10 times greater than the above-mentioned CO_2-evolution rate, a similar dependence could be seen. A precise comparison of these two kinds of surface-area dependence shows that the H_2 evolution rate for several samples, *e.g.*, NB-0, NB-5-573, NB-5-973, or NB-30, seems smaller than expected from the CO_2-evolution rate. In previous studies,[14,15,20] we have shown that the photocatalytic activity of TiO_2 for the dehydrogenation of alcohol depends on both its surface area and crystallinity, the latter of which might be a measure of e^-–h^+ recombination probability; both a larger amount of adsorbed substrates and lesser recombination are required for higher photocatalytic activity. In this sense, amorphous or hydrated TiO_2 of lower crystallinity is expected to be less active despite a relatively large surface area. On the basis of these considerations, the photocatalytic activity of Nb_2O_5 for methanol dehydrogenation, different from CO_2 evolution, should be discussed in relation to the e^-–h^+ recombination as well as the surface area. It is interesting that almost all of the TT and T crystallite samples, except for NB-5-823, showed relatively low activity. This suggests that there is a higher rate of recombination in these crystallites. On the other hand, the amorphous samples prepared *via* the solvothermal process, especially NB-5, showed the highest activity. Judging from the structural characterization shown in the previous section, we concluded that the solvothermal process in the presence of water reduces the defective sites, acting as a recombination center without excessive growth of particles, even though the structure remains in an amorphous phase.

Another possibility for the higher activity of as-prepared amorphous Nb_2O_5 powders is the negatively shifted conduction band edge as observed in the absorption spectra. In the case of TiO_2 photocatalysts, it has been shown that a small difference (*ca.* 20 nm) in the absorption edge between anatase and rutile crystallites leads to a shift in the conduction band edge.[37] The edge has been estimated for the crystalline samples to be close to the H^+/H_2 redox potential, and only a slight shift in its potential could influence the overall activity since the methanol dehydrogenation contains reduction of H^+ into H_2 by e^-. In a similar way, a difference in platinum loading must have an effect on the activity; in the present study, platinum

loading was performed by photocatalytic reaction, and shape, distribution, and other properties depend on the nature of Nb_2O_5. Since such a difference in absorption spectra or platinum deposition must be followed by changes in other physical properties, it is not clear at present which has the most significant effect on activity, but it can be stated that as-prepared amorphous Nb_2O_5 prepared by the solvothermal process in the presence of water has the highest photocatalytic activity.

Conclusions

Nb_2O_5 powders were synthesized from niobium(v) pentabutoxide by the solvothermal process in toluene at 573 K in the absence and presence of water. The phase, amorphous or crystalline, and the surface area of products could be controlled by the amount of water in the feed and through post-calcination. Water in the feed tended to crystallize and reduce the surface area, presumably due to acceleration of growth of the Nb–O–Nb network *via* a dissolution–recrystallization process. Photocatalytic activity of these samples, as well as commercial Nb_2O_5 powders, for the oxidative decomposition of acetic acid depended predominantly on their specific surface area regardless of the phase, amorphous or crystalline. The solvothermal process has the advantage of making amorphous Nb_2O_5 with a large surface area, $>200\,m^2\,g^{-1}$, which is suitable for photocatalytic oxidation. On the other hand, the activity of methanol dehydrogenation was influenced not only by the surface area but also by the phase of powders. As-prepared amorphous powder prepared by the solvothermal process in the presence of water showed the highest rate and crystallized samples showed less activity than expected from their surface area. These results suggest that Nb_2O_5 powder synthesized by the solvothermal process is amorphous but with a higher short-range order and has both a larger surface area and less defective sites, acting as a recombination site, to give the highest rate of methanol dehydrogenation among the Nb_2O_5 photocatalysts used in this study. Thus, the solvothermal process is a feasible technique for the synthesis of active Nb_2O_5 photocatalysts.

Acknowledgement

This work was partly supported by a Grant-in-Aid from the Ministry of Education, Science, Sports, and Culture of Japan (09750861, 09218202, and 09044114). Dr I. Abe and Ms Y. Yoshimura (Osaka Municipal Technical Research Institute) are acknowledged for their help in recording the Raman spectra.

References

1 N. Serpone and E. Pelizzetti, eds., *Photocatalysis: Fundamentals and Applications*, Wiley, New York, 1989.
2 A. Fox and M. T. Dulay, *Chem. Rev.*, 1993, **93**, 341.
3 M. R. Hoffmann, S. T. Martin, W. Choi and D. W. Bahnemann, *Chem. Rev.*, 1995, **95**, 69.
4 T. Watanabe, A. Kitamura, E. Kojima, C. Nakayama, K. Hashimoto and A. Fujishima, in *Photocatalytic Purification and Treatment of Water and Air*, D. E. Olis and H. Al-Ekabi, eds., Elsevier, Amsterdam, 1993. p. 747.
5 R. Wang, K. Hashimoto, A. Fujishima, M. Chikuni, E. Kojima, A. Kitamura, M. Shimohigashi and T. Watanabe, *Nature*, 1997, **388**, 431.
6 K. Sayama and H. Arakawa, *J. Phys. Chem.*, 1993, **97**, 531.
7 K. Domen, A. Kudo, A. Shinozaki, A. Tanaka, K. Maruya and T. Onishi, *J. Chem. Soc., Chem. Commun.*, 1986, 356.
8 H. Kato and A. Kudo, *Chem. Phys. Lett.*, 1998, **295**, 487.
9 Y. Inoue, T. Niiyama, Y. Asai and K. Sato, *J. Chem. Soc., Chem. Commun.*, 1992, 579.
10 Y. Nosaka, K. Yamaguchi, H. Miyama, R. Baba and A. Fujishima, *J. Photochem. Photobiol. A: Chem.*, 1992, **64**, 375.
11 M. Kanemoto, T. Shiragami, C. Pac and S. Yanagida, *J. Phys. Chem.*, 1992, **96**, 3521.
12 H. Kominami, K. Matsuo and Y. Kera, *J. Am. Ceram. Soc.*, 1996, **79**, 2506.
13 H. Kominami, K. Matsuo and Y. Kera, *J. Am. Ceram. Soc.*, 1998, **81**, 3035.
14 H. Kominami, J.-I. Kato, Y. Takada, Y. Doushi, B. Ohtani, S.-I. Nishimoto, M. Inoue, T. Inui and Y. Kera, *Catal. Lett.*, 1997, **46**, 235.
15 H. Kominami, J.-I. Kato, S. Murakami, Y. Kera, M. Inoue, T. Inui and B. Ohtani, *J. Mol. Catal. A*, 1999, **144**, 165.
16 H. Kominami, Y. Takada, H. Yamagiwa, Y Kera, M. Inoue and T. Inui, *J. Mater. Sci. Lett.*, 1996, **15**, 197.
17 H. Kominami, M. Kohno, Y. Takada, M. Inoue, T. Inui and Y. Kera, *Ind. Eng. Chem. Res.*, 1999, **38**, 3925.
18 H. Kominami, S.-I. Onoue, K. Matsuo and Y. Kera, *J. Am. Ceram. Soc.*, 1999, **82**, 1937.
19 B. Ohtani and S.-I. Nishimoto, *J. Phys. Chem.*, 1993, **97**, 920.
20 H. Kominami, T. Matsuura, K. Iwai, B. Ohtani, S.-I. Nishimoto and Y. Kera, *Chem. Lett.*, 1995, 693.
21 H. Kominami, S.-Y. Murakami, Y. Kera and B. Ohtani, *Catal. Lett.*, 1998, **56**, 125.
22 B. Ohtani, K. Iwai, H. Kominami, T. Matsuura, Y. Kera and S.-I. Nishimoto, *Chem. Phys. Lett.*, 1995, **242**, 315.
23 H. Kominami, J.-I. Kato, M. Kohno, Y. Kera and B. Ohtani, *Chem. Lett.*, 1996, 1051.
24 S.-I. Nishimoto, B. Ohtani and T. Kagiya, *J. Chem. Soc., Faraday Trans. 1*, 1985, **81**, 61.
25 JCPDS Card No. 28-0317.
26 J.-M. Jehng and I. Wachs, *Chem. Mater.*, 1991, **3**, 100.
27 M. Macek, B. Orel and U. O. Krasovec, *J. Electrochem. Soc.*, 1997, **144**, 3002.
28 B. Orel, M. Macek, J. Grdadolnik and A. Meden, *J. Solid State Electrochem.*, 1998, **2**, 221.
29 T. Ikeda and M. Senna, *J. Non-Cryst. Solids*, 1988, **105**, 243.
30 JCPDS Card No. 27-1003.
31 L. E. Brus, *Appl. Phys. A*, 1991, **52**, 465.
32 A. Henglein, *Chem. Rev.*, 1989, **89**, 1861.
33 H. Weller, *Angew. Chem., Int. Ed. Engl.*, 1993, **32**, 41.
34 K. Domen, S. Naito, T. Onishi and K. Tamaru, *Chem. Lett.*, 1982, 555.
35 S. Tearanishi, J. Nakanichi, K. Taya and K. Tanaka, *Bull. Chem. Soc. Jpn.*, 1982, **55**, 1688.
36 B. Ohtani, Y. Ogawa and S.-I. Nishimoto, *J. Phys. Chem. B*, 1997, **101**, 3746.
37 M. V. Rao, K. Rajeswar, V. R. PaiVerneker and J. DuBow, *J. Phys. Chem.*, 1980, **84**, 1987.